

Numerical Investigation of Wind Loads on Building with Various Turbulence Models

Hacımurat DEMİR*¹ 

*¹ Aksaray University, Engineering Faculty, Department of Mechanical Engineering, AKSARAY

(Alınış / Received: 07.06.2021, Kabul / Accepted: 23.07.2021, Online Yayınlanma / Published Online: 31.08.2021)

Keywords

Building aerodynamics,
Wind load,
Turbulence model,
CFD

Abstract: In this study, wind load on a building having irregular geometry was investigated numerically. In order to evaluate flow structures around the building in terms of the distributions of velocity, pressure and turbulent kinetic energy, three types of RANS models including Spalart-Allmaras one-equation, transition SST four-equation and k- ω SST two-equation models were utilized for simulation. It was evidently seen from the distributions of pressure coefficient (C_p) around surfaces of the building that positive C_p value was revealed on the west-facing of the building while north-, south-, and east-facing of the building had negative C_p for all simulation cases. By the virtue of the vortex formation in the northeast of the building, after the position of $x/L=0.7$ there was an abrupt and steep increment in C_p while on the way to the east of the building. Furthermore, it was seen from northern facing of building that suction effect was more sensitive for transition SST turbulence model compared with the others. Besides, the local highest C_p value (west-facing) was 1.364 for Spalart-Allmaras, and the maximum local suction (north-facing) was -0.892 for transition SST. Flow recirculation zone in the east-facing part of the building was the most extended for Spalart-Allmaras compared to transition SST and k- ω SST models. Looking at the positions of the spiral nodes and saddle points, there was a distinguishable difference when Spalart-Allmaras model was compared to the other models (transition SST and k- ω SST) with regard to the size of the vortex formed.

Bina Üzerindeki Rüzgar Yüklerinin Farklı Türbülans Modelleriyle Sayısal Olarak İncelenmesi

Anahtar Kelimeler

Bina aerodinamiği,
Rüzgar yükü,
Türbülans modeli,
CFD

Öz: Bu çalışmada, karmaşık geometriye sahip bir bina üzerindeki rüzgar yükü sayısal olarak incelenmiştir. Bina çevresindeki akış yapılarını hız, basınç ve türbülanslı kinetik enerji dağılımları açısından değerlendirmek için tek denklemlilik Spalart-Allmaras, dört denklemlilik transition SST ve iki denklemlilik k- ω SST olmak üzere üç tip RANS modeli simülasyon için kullanılmıştır. Tüm simülasyon durumları için bina yüzeyleri etrafındaki basınç katsayısı (C_p) dağılımlarından binanın batıya bakan cephelerinde pozitif; kuzey, güney ve doğu cephelerinde ise negatif C_p değeri olduğu açıkça görülmüştür. Binanın kuzeydoğusundaki girdap oluşumu neticesinde $x/L=0.7$ konumundan sonra binanın doğusuna doğru ilerlerken C_p değerinde ani ve dik bir artış olmuştur. Ayrıca, binanın kuzey cephesinde emme etkisinin transition SST türbülans modelinde diğerlerine göre daha duyarlı olduğu görülmüştür. Ek olarak, Spalart-Allmaras için yerel en yüksek C_p değeri (batıya bakan kısımda) 1.364 ve transition SST için maksimum yerel emme (kuzeye bakan kısımda) -0.892'ye eşittir. Binanın doğuya bakan kısmındaki akış resirkülasyon bölgesi, transition SST ve k- ω SST modellerine kıyasla Spalart-Allmaras için en geniş haldedir. Spiral düğümlerin ve semer noktalarının konumlarına bakıldığında, Spalart-Allmaras modeli diğer modellerle (transition SST ve k- ω SST) karşılaştırıldığında, oluşan girdabın boyutu açısından ayırt edici bir fark vardır.

*Corresponding Author, email: hmdemir@aksaray.edu.tr

1. Introduction

Computational fluid dynamics (CFD) is a computer-based mathematical modeling implement capable of relating to fluid flow issues and estimating physical fluid flow, heat and mass transfer, chemical reactions, and correlative phenomena by working out the mathematical equations (such as the Navies-Stokes equations) which govern these treatments utilizing numerical methods. Moreover, CFD is a combination of physics, fluid mechanics, mathematics, and computer applications. The analysis of CFD has been widely executed in numerous engineering areas where fluid behavior is an important factor, including mechanical, biomedical, wind and aerospace engineering for various applications. The utilization areas of CFD have been continuing to increase day by day. Nowadays, CFD simulations have been intensively used to perform exhaustive analyses of the interior and exterior wind environment of buildings. The branch of science in which such analyzes are conducted is called building aerodynamics. Even though the experimental surveys of the building for various wind conditions can be challenging (time, cost and scale issues and also hard to repeat in the same dynamic similarity), a full-scale model of the building modeled and analyzed in CFD provides more accurate and rapid predictions in point of various parameters such as wind flow and load. Estimations of wind pressures and forces on buildings are vital for safe and economic design. It could be a logical approach to clutch the flow around bluff body to understand the behavior of a building exposed to wind load. Because, a building has most probably the shape of a bluff body (non-streamline shape) which has sharp and flattened fronts. It is considerably executed in various engineering areas like aerospace, environment and construction, which has greater differential pressure resistance in proportion to streaklines in the event of airplane, automobiles, bridges, and building structures, etc., and also is a conventional branch in the investigation area of fluid mechanics. Highly unstable and turbulent vortices originate around the separation layers due to the sharp corners. Instabilities of pressure on bluff bodies, like buildings in natural turbulent boundary layer flows generated by intense winds, have a complicated transient and spatial structure, incurring from unstable turbulent flows in nearing wind and flow separations on the body. [1-3]

In recent years, the numbers of scientific surveys focusing on wind load behavior for low-, medium-, and complicated tall-rise buildings have been increased by researchers. Researchers have been calculated the wind load on the building utilizing various simulation techniques. It was clearly noticed that the larger part of these studies put emphasis on RANS, which is predominantly due to its well-developed specifications, less computational cost and gratifying efficiency in the industrial fields. The numerical prediction of wind flow around a rectangular plan shape building was done successfully by Mou et al [4] using RNG k- ϵ turbulent model and the distribution of the pressure around the building was investigated. The obtained result was compared with the CAARC standard models. The simulation of atmospheric boundary conditions was very much important for the wind flow around the building. Oliveira and Younis [5] had been simulated wind flow around a full-scale low-rise building with a gable roof to identify the precision of the solutions to diverse estimations. Conducting these computations with the assumption of 2D flow throughout a mid-length plane excited crucial overestimation of roof suction loads. Additionally, no separation was observed in the standard k- ϵ model, whereas Re stress closure allowed the anticipation of flow separation on the windy side of roof. Ozmen et al. [6] examined turbulent flow fields on low rise buildings with gabled roofs having varied angles both experimentally and numerically. It was seen that regions of recirculation observed on the behind of the model and leeward side of roofs because of flow separation. The numerical results indicated that for the mean pressures coefficients, standard k- ω model exhibited preferable consequences than the realizable k- ϵ turbulence model. Lien et al. [7] performed numerical simulation using various of the k- ϵ turbulence-closure model exerted with wall functions, to calculate disturbed mean flow for 2-D buildings. It was obtained that the non-linear k- ϵ model provided the ideally result between all other turbulence models investigated. Kim et al. [8] investigated the impacts of ascending amount of cross-section parts on the structural response of building models exposed to wind. It was stated that the influences of helical shape on the response characteristics reduced with rising side number, and it abated when the number of sides was 5 or more. Dagnev and Bitsuamlak [9] evaluated wind induced aerodynamic loads on CAARC building model considering the impact of neighboring building. A convenient agreement has been observed mean pressure coefficients between wind tunnel and numerical results.

Sharma et al. [10] comprehensively reviewed both minor and major aerodynamic modifications broadly. Structures having bluff shape were more tender to heavy wind-induced stimulations and could be handled with modifications such as aerodynamic or structural. It was seen that these modifications altered the wake dynamics and vortex shedding incident. Chamfering, corner cut and rounding modifications cultivated the reattachment of shear layer and attenuated the wake width on back side of the building. Further, the researchers continued with the detailed review of shape modifications in buildings such as curve corners and major modifications such as altering the building shape and elevation. Xie [11] asserted a convenient approximation to determine efficacy of aerodynamic methods employed to reduce effect of wind such as tapering, twisting and stepping. Daemei et al. [12] investigated wind aerodynamics and flow behaviours of triangular models with various aerodynamic variations including rounded, recessed and chamfered corners numerically. It was found that rounded-corners, tapered led to drag coefficient decline of the building. Tanaka et al. [13] investigated the effect of various aerodynamic modifications on a square shaped tall building to measure aerodynamic forces and wind pressures

experimentally. Bhattacharya and Dalui [14] performed both numerical and experimental studies for the dispersion of pressure on E-shaped plan under wind excitation. They obtained that in order to calculate mean pressure coefficients, as a result of comparison, SST $k-\omega$ turbulence model gave better results than the $k-\epsilon$ turbulence model. At skew wind angles, the maximal positive and negative mean pressures of some faces of the building are supplied. Zhao Liu et al [15] performed a twisted wind flow on a square mega tall building using wind tunnel test and the results of pressure distribution are studied. Tamura and Miyagi [16] investigated the effect of various corner modifications on a square cylinder considering laminar and turbulent flow conditions experimentally in order to establish physical mechanism of the decline in wind load on high-rise building. They stated that rounded and chamfered corners decreased drag forces, due to the reduction in width of wake. Tominaga et al. [17] performed both numerically and experimentally study about airflow around buildings having isolated gable roof with various pitches. There was good agreement between the CFD results and measured values for the streamwise velocity. The focus of the recirculation eddy back the roof proceeded uphill and wander away the building with an ascent in the pitch of roof. For all of the roof pitches, the maximum value of turbulent kinetic energy observed around the downstream eaves. Increase in pitches of the roof caused to decrease in these values.

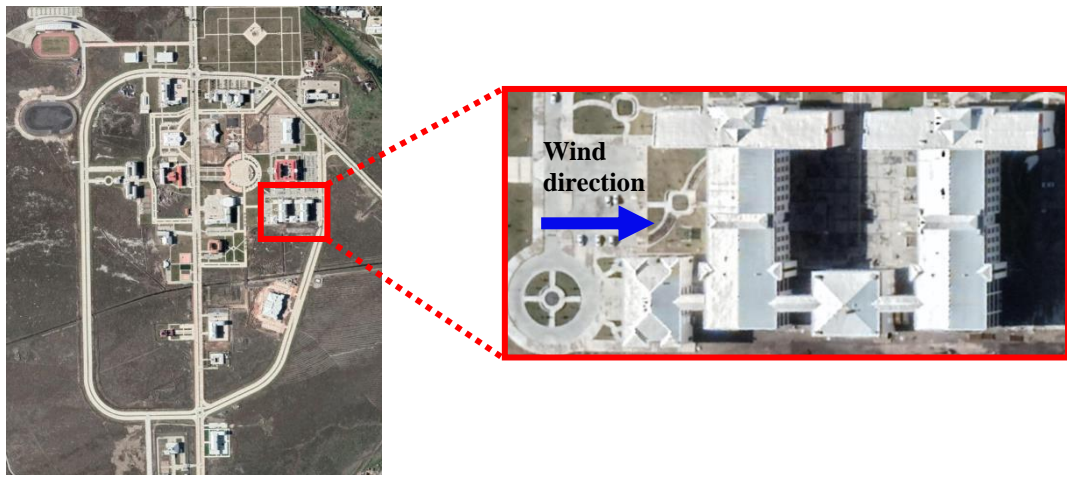
Özkan et al. [18] and Blocken et al. [19] focused on the wind load and wind speed distributions. For various passage widths, Blocken et al. [19] investigated wind speed situations in passages between parallel buildings. In order to examine flow around the building, $k-\epsilon$ turbulence model was selected and applied. Obtained results from the simulation demonstrated that the rise of wind speed in passages was only noticed at the pedestrian level and that the flow rate across the passage was chiefly 8% greater than the flow rate of the free field. The impacts of side ratio on wind-induced pressure distribution on rectangular shape buildings were examined by Amin and Ahuja [20]. It was stated that the distribution and magnitude of wind pressure on sidewalls and leeward walls were noticeably influenced by the side ratio of building. However, it had a tiddly effect on windward walls as wind direction was parallel to the roof ridge. Nozawa and Tamura [21] performed a numerical study to investigate flow around the low-rise building immersed in turbulent boundary layers. It was stated that the elusion from minimum pressure on the roof and the sides was vigorously influenced by the turbulence of nearing flows.

When the existing literature regarding this study is surveyed, it is noticed that while the studies investigating the flow fields on building models with simple geometry stand out, there are not many studies that examine the wind flow in complex and irregular-shaped buildings using different turbulence models. In this context, this study mainly focuses on the wind load around an irregular-shaped building under the wind flow using various turbulence models.

2. Material and Method

2.1. Numerical Method

The two-dimensional, steady-state, numerical simulation has been performed with solving Reynolds Averaged Navier-Stokes Equation (RANS) equations by using the ANSYS Fluent software for existing building of the Engineering Faculty located in Aksaray University. COUPLED algorithm scheme was utilized to solve discretized equations for the pressure-velocity coupling. On spatial discretization, in order to compute the gradient, the least-squares cell-based method has been selected besides the second-order upwind method has been employed for all further parameters. Figure 1 shows the top view of the main campus environment of Aksaray University from Google Earth and Figure 1b shows the zoomed-in layout of the Engineering Faculty's building which is selected for the simulation. Figure 2 delineates the computational domain of CFD simulation and its dimensions with regard to length of the building. In order to construct computational domain properly according to the recommendation given by Bartzis et al. [22] and Franke et al. [23], the building was positioned to 5L far from the inlet and 15L from the outlet. Furthermore, the clearances of north and south directions were situated five times the length of the building. In the present numerical study, quadrilateral dominant type mesh was constructed (as can be seen in Figure. 3) and three different mesh types were used to obtain grid-independent results, and approximately 0.4 million computational grids were chosen for comprising the simulation circumstances in line with the results given in Table 1. Boundary layer was constructed considering smooth transition with growth factor 1.2 and total layer is 5. Convergence of the computations was obtained for both continuity and momentum equations when residuals were lower than 10^{-5} .



a) b)
Figure 1. Overview of the Aksaray University campus buildings.
 a) main campus b) building of Engineering Faculty

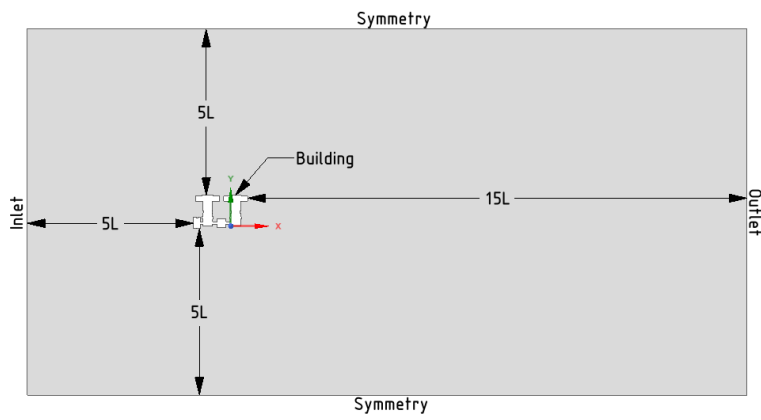


Figure 2. Dimensions of computational domain and boundary conditions.

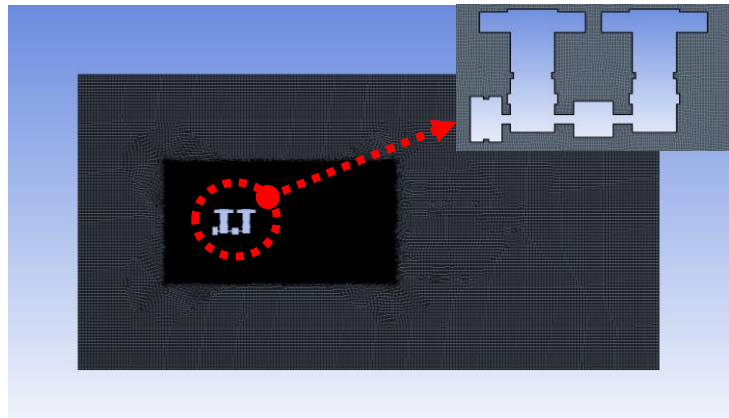


Figure 3. Mesh structure around the building.

Table 1. Details of different mesh schemes

Mesh scheme	Number of nodes	C_D
1	0.38 million	1.7047601
2	0.40 million	1.7188737
3	0.52 million	1.7189921

3. Results

3.1. Pressure Distribution around the Building

In order to evaluate wind loads on the structures, knowledge of external distribution is vital. The distributions of pressure around the building are investigated for various turbulence models in this study. The pressure coefficient (C_p) is a nondimensional parameter, found using equation 1.

$$C_p = \frac{P - P_0}{\frac{1}{2} \rho U^2} \tag{1}$$

where ρ is density of air, P is the local pressure on the building surface, P_0 is the far upstream pressure and U is velocity of wind.

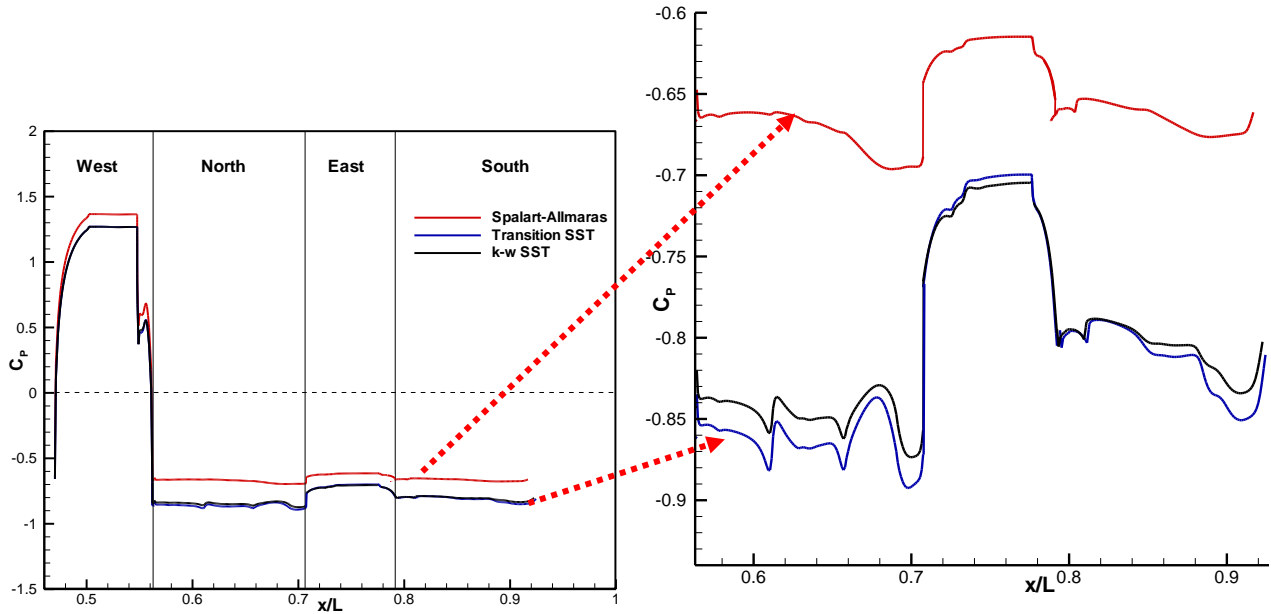


Figure 4. Distributions of pressure coefficients for the building obtained by different turbulence models.

Figure 4 represents the distributions of pressure coefficient (C_p) around surfaces of the building at 1 m/s wind speed are given comparatively with the results of Spalart-Allmaras, transition SST and $k-\omega$ SST turbulence models. When the variations of C_p around the building calculated using different turbulence models are examined, it can be seen that there is similar characteristic behavior of the variations of C_p . West-facing of the building is exposed to positive C_p , whereas north-, south-, and east-facing are exposed to negative C_p . As shown in Figure 4, pressure distributions on west-facing of the building are almost the same in each case while the pressure distributions on the other directions from $x/L=0.56$ to 0.92 are different for each case with 1m/s. In order to examine the differences and similarities between the C_p values for all three cases, the graphic lines are magnified and the pressure distributions on the north, south and east facing parts of the building are more clearly visible. As can be seen from the study of Mou et al. [4], it is interesting to note that wind pressures on east-facing of the building (leeward wall) were quite stable, lying in a horizontal line. Furthermore, wind pressures on the north- and south-facing of building happened considerable fluctuations, in order to make a slow transition from the north- and south-facing (sides) to east facing (leeward) in negative pressure. Additionally, it is seen that there is a sudden and step increase in the pressure coefficient while moving to the east of the building due to the vortex occurring in the northeast of the building after the position of $x/L=0.7$. In general, when the pressure coefficient values calculated around the building are examined due to the 1 m/s wind blowing from the west of the building, it is seen that the Spalart-Allmaras model is larger than other turbulence models. Besides, it is seen from northern facing of building that suction effect is more critical for transition SST turbulence model compared with the others. From the analysis of wind C_p of building, it is stated that the local highest C_p value (west-facing) is 1.364 for Spalart-Allmaras, and the maximum local suction (north-facing) is -0.892 for transition SST.

3.2. Drag Coefficient around the Building

Wind is a horizontal air movement generated by pressure differences between air masses and air flows from high pressure region to low pressure region. In other words, wind can be defined as main force acting on structures, buildings etc. horizontally, that is proportionate to the drag coefficient. For structural and aerodynamic designs, drag coefficient is considerable parameter. In order to measure the drag coefficient of buildings experimentally is both time-consuming and expensive. In this study, drag coefficients are computed by using CFD for a building in Aksaray University considering the actual geometry of building.

To evaluate the drag quantity (drag force) or resistance of an object against a fluid flow such as air or water, a dimensionless parameter drag coefficient which is indicated as C_D in fluid dynamics is addressed. C_D is calculated using below equation;

$$C_D = \frac{F_D}{\frac{1}{2} \rho U^2 A} \quad (2)$$

where ρ is density of air; F_D is average drag force; and A is the reference area of the building.

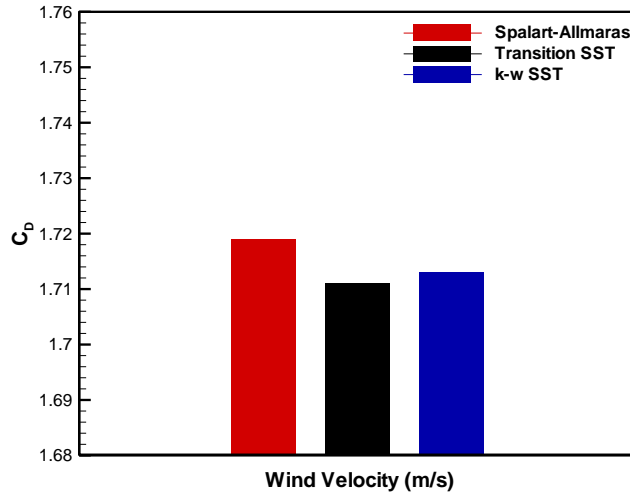


Figure 5. Comparison of drag coefficient obtained by numerical simulation.

Figure 5 shows the drag coefficient (C_D) obtained from numerical study at constant wind velocity of 1m/s for three different turbulence models. It was computed as 1.719 by the Spalart-Allmaras, 1.711 by the transition SST model, and 1.713 by k- ω SST model, respectively. By the virtue of decline in wake width, drag force exerted on the building decreased.

3.3. Flow Field Visualization

Figure 6 shows the streamlines superimposed onto the non-dimensional velocity contours. The velocity contours with streamline resulting from each turbulence model investigated in this work are depicted for the whole wind flow field around the building as can be seen in Figure 6. It is clear that all three cases share the same streamline profile, including two symmetrically rotating vortices in clockwise and counterclockwise directions. These vortices that were formed in the east-facing part of the building include spiral nodes (F_1 and F_2) and one saddle point (S). In Figure 6a, for the Spalart-Allmaras case, the saddle point (S) that represents the location of end point of the circulation zone of the vortex is located at $x/L = 11.95$ and a pair of recirculation nodes centered at $x/L = 7.81$. Similarly, Figure 6b, presents a saddle point at $x/L=7.87$ and a pair of recirculation nodes at $x/L=5.48$ for transition SST case. On the other hand, saddle point equals to $x/L=7.91$ and location of recirculation is at $x/L=5.58$ for k- ω SST case. Looking at the positions of the spiral nodes and saddle points, there is a distinguishable difference when Spalart-Allmaras model is compared to the other models (transition SST and k- ω SST) with regard to the size of the vortex formed. Flow recirculation zone in the east-facing part of the building is the largest for Spalart-Allmaras case comparing with other cases. As stated before, drag force exerted on the building diminished as a result of reduction in wake width.

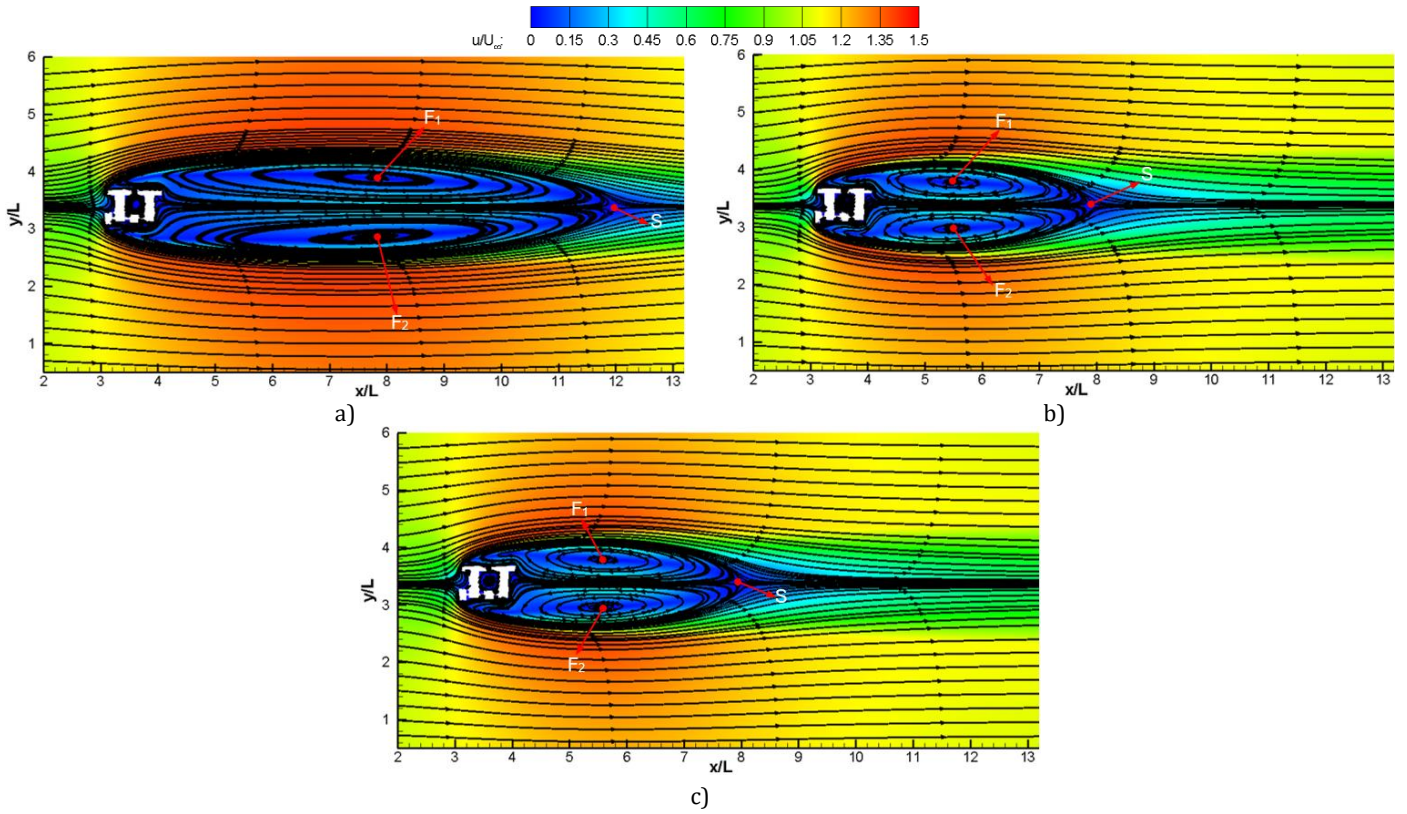
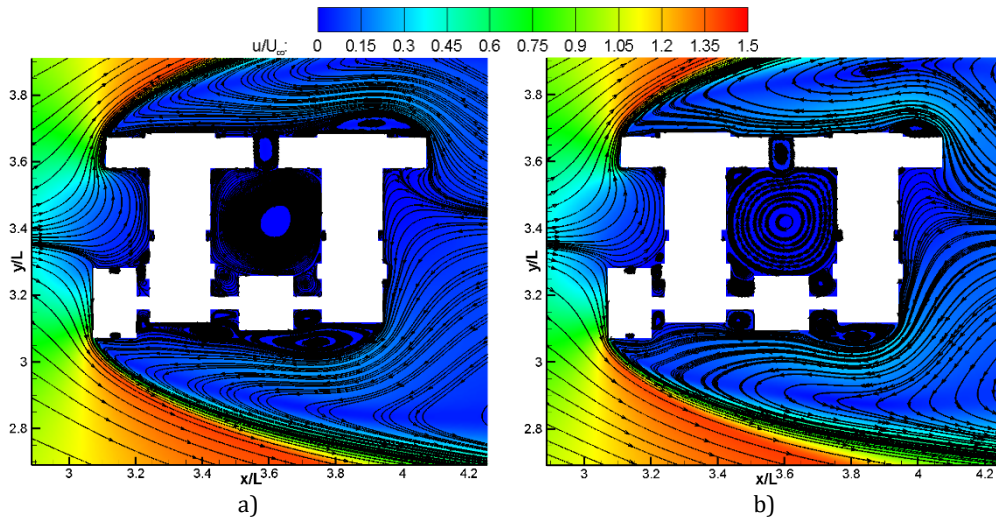


Figure 6. Non-dimensional velocity distribution contour together with streamlines for different turbulence models. a) Spalart-Allmaras b) transition SST c) $k-\omega$ SST



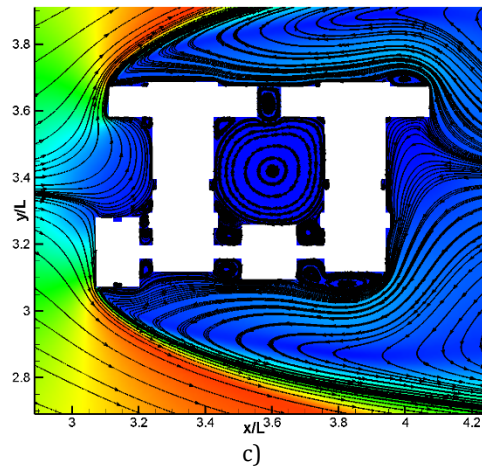


Figure 7. A close-up view of the flow patterns around the building.
 a) Spalart-Allmaras b) transition SST c) k- ω SST

It can be observed that the major parts of wind flow pattern around the building are similar, which are demonstrated in Figure 7 for Spalart-Allmaras, transition SST and k- ω SST turbulence models, respectively. A few unusual behaviours are observed at northeast-facing of and south-facing of the building; the size of secondary vortex is the largest for Spalart-Allmaras case. Additionally, it is seen that the wind flow coming from the western part of the building turns north and south from the stop point and separates from the corners of the west-facing part of the building. Small-scale eddies occurred on the north and south-facing surfaces parallel to the flow. The flow diverging from the north-facing part of the building caused the formation of a small counterclockwise vortex at the north-right corner of the building. The behaviors of the flow that occurred in the middle of the building were similar to lid-driven cavity flow. As can be seen from Figure 7, as large clockwise-rotating primary vortices formed in the geometric center of the interior of the building, counter-clockwise rotating secondary eddies occurred at the three corners of the bottom left, bottom right, and top left. Additionally, the clockwise-rotating small tertiary eddies formed at the top right corner of the building.

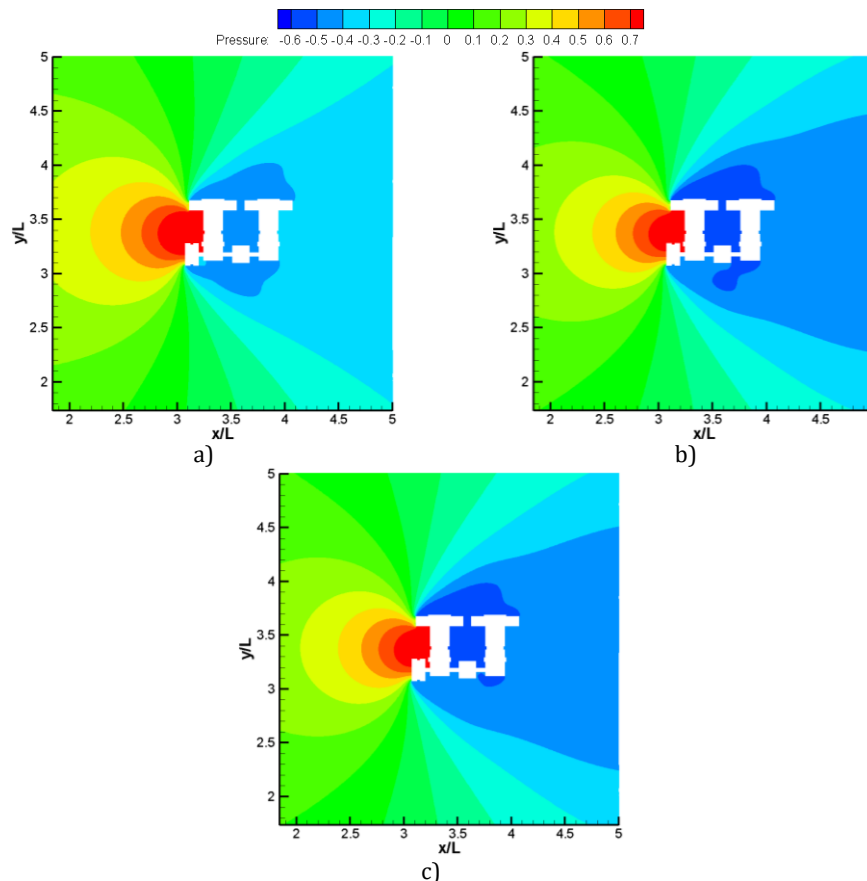


Figure 8. Pressure distribution contour for different turbulence models.
 a) Spalart-Allmaras b) transition SST c) k- ω SST

The distributions of wind pressure coefficients (C_p) of the building resulting from each turbulence model are shown in Figure 8. As seen from the contours of C_p on the building for all turbulence models are similar; the only remarkable distinction is their shape which acts the pressure distribution over the southern facing of building. Since the structure of the building is dissymmetrical, the pressure distribution of this building differs in every direction and the maximum value of C_p is observed at the west-facing (stagnation point) of the building.

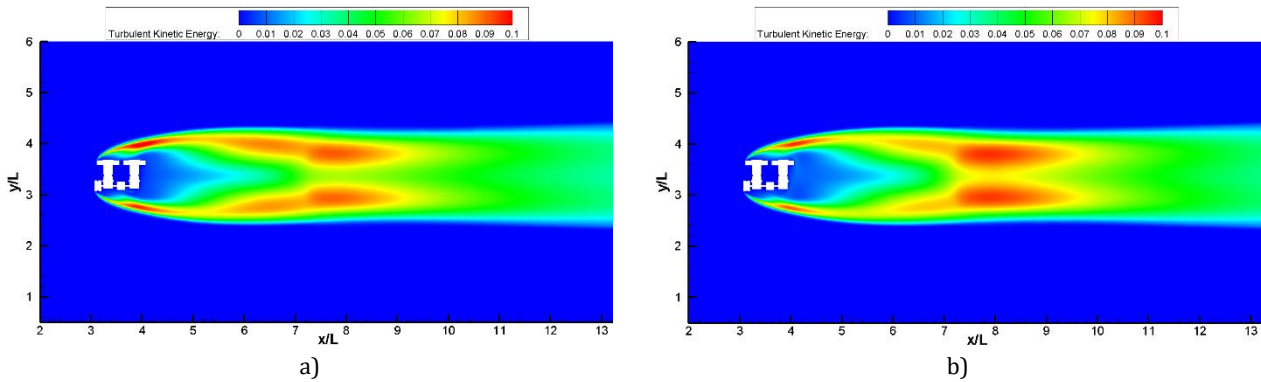


Figure 9. The turbulent kinetic energy distributions around the building.
a) transition SST b) $k-\omega$ SST

In the following section, the comparison of turbulent kinetic energy (TKE) in the flow field is depicted. The contours show that the generation of TKE is about the shear in the flow arising from the building. The distribution of the turbulent quantities is found clearly symmetric along the $y/H=3.4$ axis. It is clear that the peak value of TKE appears at the shear layer and lies streamwise between the end of the vortex formation region and wake recirculation region, particularly around the saddle point. In fact, as observed in Figure 9, TKE has no considerable deviation between transition SST and $k-\omega$ SST. Only one difference is the maximum region of TKE value located behind the end of the recirculation area for transition SST is smaller than $k-\omega$ SST in the wake region.

4. Discussion and Conclusion

In this study, the numerical simulation has been carried out to evaluate the wind load on the selected irregular shape building using Spalart-Allmaras, transition SST and $k-\omega$ SST turbulence models under the same condition and constant wind velocity. As a consequence of pressure distributions given in Figure 4, one can realize that pressure coefficients (C_p) occurring along the building obtained by using Spalart-Allmaras is greater than those obtained with other turbulence models. It is observed that the pressure distribution on the west-facing of building is similar for all the turbulence models studied. The wind pressures on east-facing of the building were quite stable, lying in a horizontal line. Wind pressures on the north- and south-facing of building happened considerable fluctuations, in order to make a slow transition from the north- and south-facing to east facing in negative pressure. Considering the results obtained for the northern facade of the building, it was understood that the suction effect is more sensitive in the transition SST turbulence model compared to other models. Besides, the maximum local suction value of C_p (north-facing) is equal to -0.892 for transition SST whereas the maximum local value of C_p (west-facing) is equal to 1.364 for Spalart-Allmaras. In addition to this, the drag coefficient (C_D) was computed as 1.711 by the transition SST model, 1.713 by $k-\omega$ SST model, and 1.719 by the Spalart-Allmaras, respectively. It is obvious that the same streamline profile occurred which has two symmetrically rotating vortices in clockwise and counterclockwise directions for all three cases. Flow recirculation zone in the east-facing part of the building is the most extended for Spalart-Allmaras situation compared to other situations. Additionally, there is a remarkable distinction in point of size of vortices formed in the Spalart-Allmaras model is compared to transition SST and $k-\omega$ SST models. It was also revealed that the generation of TKE caused by the shear in the flow arising from the building was found clearly symmetric along the $y/H=3.4$ axis. It is concluded that the ultimate value of TKE appears at the shear layer and lies streamwise between the end of the vortex formation region and the wake recirculation region, especially around the saddle point. As stated before in Fig. 9, the maximum region of TKE value located behind the end of the recirculation zone for transition SST is less than $k-\omega$ SST in the wake region.

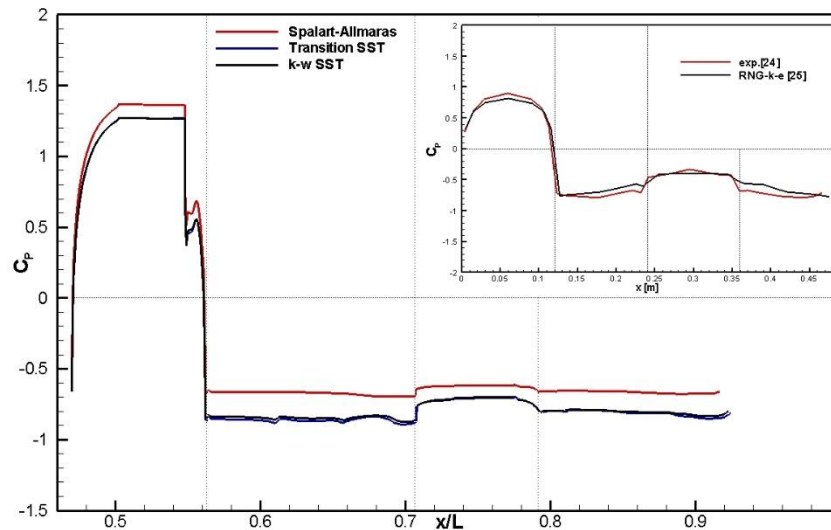


Figure 10. Comparison of the C_p distributions around the building.

In connection with the variation of C_p , when comparing the findings of this study with the literature of [24] and [25], although both the wind value and the shape of buildings are not exactly same, C_p distributions around the building indicate similar trends. At the same time, it is concluded from this comparison graph that the positive pressure coefficients occurred on the windward wall (west-facing in this study), which was directly exposed to the wind flow, due to the pushing effect, and negative pressure coefficients occurred on the side (north and south facing) and leeward (east-facing) walls because of the suction effect as illustrated in Figure 10.

Acknowledgment

The author would like to thank all his colleagues in Wind Engineering and Aerodynamics Research Group (WEAR) at Erciyes University for allowing the use of ANSYS software.

References

- [1] Versteeg, H. K., & Malalasekera, W. 2007. An introduction to computational fluid dynamics: the finite volume method. Pearson education.
- [2] Holmes, J. D. 2018. Wind loading of structures. CRC press. New York: Taylor & Francis Group
- [3] Zhao, M. 2021. Prediction and Validation Technologies of Aerodynamic Force and Heat for Hypersonic Vehicle Design. Springer Nature.
- [4] Mou, B., He, B. J., Zhao, D. X., & Chau, K. W. 2017. Numerical simulation of the effects of building dimensional variation on wind pressure distribution. *Engineering Applications of Computational Fluid Mechanics*, 11(1), 293-309.
- [5] Oliveira, P. J., & Younis, B. A. 2000. On the prediction of turbulent flows around full-scale buildings. *Journal of Wind Engineering and Industrial Aerodynamics*, 86(2-3), 203-220.
- [6] Ozmen, Y., Baydar, E., & Van Beeck, J. P. A. J. 2016. Wind flow over the low-rise building models with gabled roofs having different pitch angles. *Building and Environment*, 95, 63-74.
- [7] Lien, F. S., Yee, E., & Cheng, Y. 2004. Simulation of mean flow and turbulence over a 2D building array using high-resolution CFD and a distributed drag force approach. *Journal of Wind Engineering and Industrial Aerodynamics*, 92(2), 117-158.
- [8] Kim, Y. C., Bandi, E. K., Yoshida, A., & Tamura, Y. 2015. Response characteristics of super-tall buildings—Effects of number of sides and helical angle. *Journal of Wind Engineering and Industrial Aerodynamics*, 145, 252-262.
- [9] Dagnev, A. K., & Bitsuamlak, G. T. 2010. LES evaluation of wind pressures on a standard tall building with and without a neighboring building. *The Fifth International Symposium on Computational Wind Engineering (CWE2010) Chapel Hill, North Carolina, USA May 23-27.*

- [10] Sharma, A., Mittal, H., & Gairola, A. 2018. Mitigation of wind load on tall buildings through aerodynamic modifications. *Journal of Building Engineering*, 18, 180-194.
- [11] Xie, J. 2014. Aerodynamic optimization of super-tall buildings and its effectiveness assessment. *Journal of Wind Engineering and Industrial Aerodynamics*, 130, 88-98.
- [12] Daemei, A. B., Khotbehsara, E. M., Nobarani, E. M., & Bahrami, P. 2019. Study on wind aerodynamic and flow characteristics of triangular-shaped tall buildings and CFD simulation in order to assess drag coefficient. *Ain Shams Engineering Journal*, 10(3), 541-548.
- [13] Tanaka, H., Tamura, Y., Ohtake, K., Nakai, M., & Kim, Y. C. 2012. Experimental investigation of aerodynamic forces and wind pressures acting on tall buildings with various unconventional configurations. *Journal of Wind Engineering and Industrial Aerodynamics*, 107, 179-191.
- [14] Bhattacharyya, B., & Dalui, S. K. 2020. Experimental and numerical study of wind-pressure distribution on irregular-plan-shaped building. *Journal of Structural Engineering*, 146(7), 04020137.
- [15] Liu, Z., Zheng, C., Wu, Y., Flay, R. G., & Zhang, K. 2019. Investigation on the effects of twisted wind flow on the wind loads on a square section megatall building. *Journal of Wind Engineering and Industrial Aerodynamics*, 191, 127-142.
- [16] Tamura, T., & Miyagi, T. 1999. The effect of turbulence on aerodynamic forces on a square cylinder with various corner shapes. *Journal of Wind Engineering and Industrial Aerodynamics*, 83(1-3), 135-145.
- [17] Tominaga, Y., Akabayashi, S. I., Kitahara, T., & Arinami, Y. 2015. Air flow around isolated gable-roof buildings with different roof pitches: Wind tunnel experiments and CFD simulations. *Building and Environment*, 84, 204-213.
- [18] Özkan, R., Sen, F., & Ballı, S. 2020. Evaluation of wind loads and the potential of Turkey's south west region by using log-normal and gamma distributions. *Wind and Structures*, 31(4), 299-309.
- [19] Blocken, B., Carmeliet, J., & Stathopoulos, T. 2007. CFD evaluation of wind speed conditions in passages between parallel buildings-effect of wall-function roughness modifications for the atmospheric boundary layer flow. *Journal of Wind Engineering and Industrial Aerodynamics*, 95(9-11), 941-962.
- [20] Amin, J. A., & Ahuja, A. K. 2013. Effects of side ratio on wind-induced pressure distribution on rectangular buildings. *Journal of Structures*.
- [21] Nozawa, K., & Tamura, T. 2002. Large eddy simulation of the flow around a low-rise building immersed in a rough-wall turbulent boundary layer. *Journal of Wind Engineering and Industrial Aerodynamics*, 90(10), 1151-1162.
- [22] Bartzis, J. G., Vlachogianis, D., & Stefanos, A. 2004. Best Practice Advice for Environmental Flows. TA5 QNET CFD network Newsletter, 2(4).
- [23] Franke, J., Hellsten, A., Schlünzen, H., & Carissimo, B. 2007. Best practice guideline for the CFD simulation of flows in the urban environment. COST action 732. Quality Assurance and Improvement of Meteorological Models. University of Hamburg, Meteorological Institute, Center of Marine and Atmospheric Sciences.
- [24] Hunte, S. 2010. Testing the application of CFD for building design. Delft University of Technology, Master Thesis, Netherland.
- [25] Özmen, Y., & Kaydok, T. 2014. Kare kesitli bir yüksek bina üzerindeki türbülanslı akışın sayısal olarak incelenmesi. *Kahramanmaraş Sutcu Imam University Journal of Engineering Sciences*, 17(2), 15-25.